Trust Regions in Surrogate-Assisted Local Search for Industrial Columns' Mass Transfer Efficiencies Estimation

Miaomiao Qu
Faculty of electrical engineering and computer science
Ningbo University
Ningbo, China
qumiaomiao@nbu.edu.cn

Jian Wang
Faculty of electrical engineering and computer science
Ningbo University
Ningbo, China
wangjian@nbu.edu.cn

Xuhua Shi
Faculty of electrical engineering and computer science
Ningbo University
Ningbo, China
shixuhua@nbu.edu.cn

Xiaoxia Chen
Faculty of electrical engineering and computer science
Ningbo University
Ningbo, China
chenxiaoxia@nbu.edu.cn

***Abstract*—Tray efficiencies are important structural parameters for distillations' modeling and optimization. However, determining tray efficiencies in industrial practice remains a challenge. A new method of estimating tray efficiencies by using industrial operating data is proposed in this study. The proposed approach called trust regions in surrogate-assisted local search (TRSALS) is developed on the basis of industrial operating data. In TRSALS, the tray efficiencies are estimated by solving a constrained optimization problem, which is based on the combination of Kriging surrogate based global search and RBF surrogate-based trust-region local search. The estimated key tray temperature profile is compared with that of the actual one of the industrial column to verify the feasibility of the proposed method. Experimental results show that the performance of TRSALS was outstanding compared with that of a Kriging surrogate-only-based algorithm.**

Keywords—trust region, evolutionary optimization, distillation column, Murphree efficiency

I. INTRODUCTION

Fractionation distillation unit is a common equipment in the petrochemical industry, which plays an important role in process production [1,2]. It is necessary to simulate the distillation operation processes to make full use of the resources, optimize the operation of the device, and reduce the energy consumption and cost [3,4]. It is known that only physical changes are involved in the fractionation processes. Modeling of the fractionation process is established by the material balance, phase balance, molar fraction addition, and enthalpy balance [5]. However, the Murphree efficiencies of the actual fractionation unit will change with the operation cycle and raw material condition, which will bring difficulties to the accurate establishment of fractionation models. Therefore, it is an important task for petrochemical enterprises to explore an effective approach to estimation of the mass-transfer efficiencies of the distillation, to establish a fractionation model in line with the actual industry, and to find the best operating parameters of the fractionation unit according to the raw material properties and product quality requirements, so as to reduce production costs and energy consumption and to improve economic benefits [6].

Generally, two kinds of models, namely, theoretical and empirical, are used for tray efficiencies' estimation. Theoretical models are based on the internal mechanism of the distillation processes or mass transfer, and the cross-flow hydraulic effects on the tray. The most influential theoretical model is based on the experiments that are conducted on a tray with a small bubble cap, termed the American Society of Chemical Engineers (AIChE) method [7]. In view of some unreliability of the AIChE method, Refs. [8–12] contain several modifications that provided more satisfactory fitting for some experimental research. Regarding the theoretical model of a tray column, the relationship between mass-transfer area, tray specifications, system physical properties, and operating conditions are complex and not yet sufficiently well understood [13]. Furthermore, the numerical simulations are very complex and time-consuming, while empirical models are data driven and have been developed to describe experimental efficiencies in terms of the physical properties, tray geometry, and operating conditions. An empirical correlation for global efficiency was proposed in Ref. [14], which is widely used in the industry because of its simplicity, and in Ref. [15], an approach predicting the sieve tray efficiency using neural networks was provided. Other empirical approaches are described in Refs. [16–18]. However, the empirical models are difficult to generalize in industrial applications because of simple relationship between tray efficiency and other factors. In addition, the prediction results may be inaccurate because of the limited number of experiments. Therefore, the estimation of tray efficiency remains a challenge.

The main idea of this study was to establish an appropriate method of estimating the tray efficiencies of industrial distillation columns. Different from the previous empirical and theoretical models, the tray efficiencies are estimated by solving a constraint evolutionary optimization problem, which is based on the combination of Kriging surrogate-based global searching and RBF surrogate-based trust-region local search. A new method called trust regions in surrogate-assisted local search (TRSALS) is developed on the basis of a certain amount of industrial operating data. Finally, the estimated key tray temperature profile is compared with that of the actual one

978-1-7281-6929-3/20/$31.00 ©2020 IEEE

of the industrial column to verify the feasibility of the proposed method.

The rest of this paper is organized as follows: Section 2 presents the description of the tray estimation problem. Section 3 details the main steps of the proposed algorithm, and Section 4 presents several experimental results in the application of Murphree efficiency determination of the distillation column. Concluding remarks are given in Section 5.

II. Problem Statement

Theoretically, the Murphree efficiencies can be expressed as follows:

$$Eff_{i,j}^{M} = \frac{Y_{i,j} - Y_{i,j+1}}{K_{x,y}X_{i,j} - Y_{i,j+1}} \tag{1}$$

where Eff^{M} is the Murphree efficiency, K the equilibrium constant, X the liquid-phase mole fraction, Y the vapor-phase mole fraction, and i and j represent the ith component and the jth tray, respectively.

As the experimental data of Murphree efficiencies are difficult to directly obtain without collection of samples from the stage outlets during the industrial process, in this study, the tray efficiencies are chosen by checking the temperature profile obtained via simulation against the corresponding measurements of the industrial columns. The actual temperature distribution of the trays can indirectly characterize the separation efficiency of the distillation columns. Hence, the estimation of the tray efficiency can be transformed into a solution of an inequality-constrained evolutionary optimization problem as follows:

$$\begin{aligned} &f(\mathbf{x}) = min\sum_{j}\left(\frac{T_j - \hat{T}_j(\mathbf{x})}{T_j}\right)^2 \\ &\text{Subject to } g_i(\mathbf{x}) \le 0 \quad i = 1,2,\cdots,m \end{aligned} \tag{2}$$

where $\mathbf{x}$ are the decision variables of the problem, represented the tray Murphree efficiencies for the researched tower, j is the tray number with a temperature measuring point, T is the measured tray temperature (°C), and $\hat{T}$ is the calculated tray temperature (°C). Typically, the distillation unit has more than 50 plates. The global optimal solution for high-dimensional and highly nonlinear problems can be searched by adjusting the tray efficiency to obtain the minimum $f(\mathbf{x})$ in Formula (2). $g(\mathbf{x})$ are the constraints for the problem, considering some restrictions on the product quality and safety of the tower. Owing to the constraints, when evaluating a decision vector $\mathbf{x}$, its degree of constraint violation is considered. The degree of constraint violation of $\mathbf{x}$ can be computed as follows:

$$V(\mathbf{x}) = \sum_{i=1}^{m} V_i(\mathbf{x}) \tag{3}$$

$$V_i(\mathbf{x}) = \max(0, g_i(\mathbf{x})), i = 1,2,\cdots,m \tag{4}$$

$V(\mathbf{x}) > 0$ indicates that the constraint is violated. The larger the violation $V(\mathbf{x})$, the larger the penalty should be; if $V(\mathbf{x}) = 0$, the violation is not violated.

III. Trust Regions in Surrogate-Assisted Local Search

There are some complex factors affecting tray efficiency, such as plate structure, manipulation conditions, and the varying nature of the physical systems in use, which can lead to deviations from the theoretical trays' models. Figure 1 is a flowchart that shows the main steps of the TRSALS algorithm. The algorithm begins by initializing the parent population with Latin hypercube design, and then calculates the columns' objective and constraint functions, which are listed in Eq. (2) at the initial population. TRSALS then goes through a main loop that terminates when the computational budget (the maximum number of evolutionary generations in this paper) is reached. In the first part of the loop, TRSALS fits the surrogates (Kriging as well) for the objective and constraint functions, and generates a large number of trial offspring for each parent, and then uses the surrogates to select only the most promising trial offspring, which should be satisfied Eq. (5) in the entire decision space:

$$\begin{aligned} &x_t^{\exp} = \arg\max(\mathrm{E(I)}\left| f_{Su-g}(\mathbf{x}, D_g(t))\right.) \\ &s.t.\ \ \mathbf{g}_i(\mathbf{x}) < 0, i = 1,2,\cdots,m \end{aligned} \tag{5}$$

In the second part of the loop, the refinement of the best parent solution in this study is implemented by solving the trust-region sub-problem, which can be expressed as follows:

$$\min_{\mathrm{p}\in \mathrm{R}^{\mathrm{n}}} \widetilde{f}_{\mathrm{t}}(\mathbf{p}) = f(k) + \mathbf{d}_t^T\mathbf{p} + \frac{1}{2}\mathbf{p}^T B_t\mathbf{p},\ \text{s.t.}\|\mathbf{p}\| \le \Delta_t \tag{6}$$

where $\mathbf{p}$ are the searching steps, $d_t = \nabla f(x_t)$, $B_t = \nabla^2 f(x_t)$, and Δ_t is the trust-region radius. The surrogates (RBF as well) are constructed using information from recently evaluated points, and when the trust-region sub-problem is solved, the function evaluations are performed on the solution to the trust-region subproblem, the algorithm parameters and the trust region are updated, and, at the termination time, the best solution is achieved. Hence, following two main points are important in the process of surrogate modeling and searching: (1) to select the most promising among multiple trial offspring for each parent solution, and (2) to identify a local refinement point for the current best solution during the trust-region step. The main steps of the TRSALS algorithm are the following:

(1) Set the generation counter $t = 0$ and generate the initial population $\mathbf{x}_0 = \{x_1(0), x_2(0), \cdots, x_N(0)\}$ by Latin hypercube design.

(2) Calculate the values of the original objective and constraint function at the points in $\mathbf{x}_0$: $\{f_{i,t}, g_{i,t}, i = 1,2,\cdots N\}$.

(3) Initialize dataset: $D_t = \{x_{i,t}, f_{i,t}, g_{i,t}, i = 1,2,\cdots N\}$.

(4) While the termination criteria are not satisfied, do the following:

(4.1) Fit/update the Kriging model by utilization all the individuals in D_t to approximate the original objective and constraint functions $M_t = \{S_t, \mathbf{G}_{t,j}\}, j = 1,2,\cdots,m$.

(4.2) For each individual $\mathbf{x}_t$ in D_t.

(4.3) Generate the most uncertain individual A_t of S_t by surrogate-assisted search using a traditional particle swarm optimization algorithm with feasibility constraint rules.

(4.4) Compute the original objective and constraint functions at the point $A_t : \{f(A_t), \mathbf{g}(U_t)\}$ and update dataset D_t.

(4.5) Update S_t for the objective and constraint functions $M_t = \{S_t, \mathbf{G}_{t,j}\}, j = 1,2,\cdots,m$ separately using newly obtained function values from simulations on the current offspring.

(4.6) Compare A_t with $\mathbf{x}_t$ according to the feasibility rule, and select the better one into dataset D_t.

(4.7) Select the best individual A_t' in D_t.

(4.8) Compute the original objective and constraint functions at the point $A_t' : \{f(A_t'), \mathbf{g}(A_t')\}$, and update dataset D_t.

(4.9) If A_t' is in the feasibility region, execute the *RBF-TR* algorithm, t=t+1.

End While

(5) Return the best solution found.

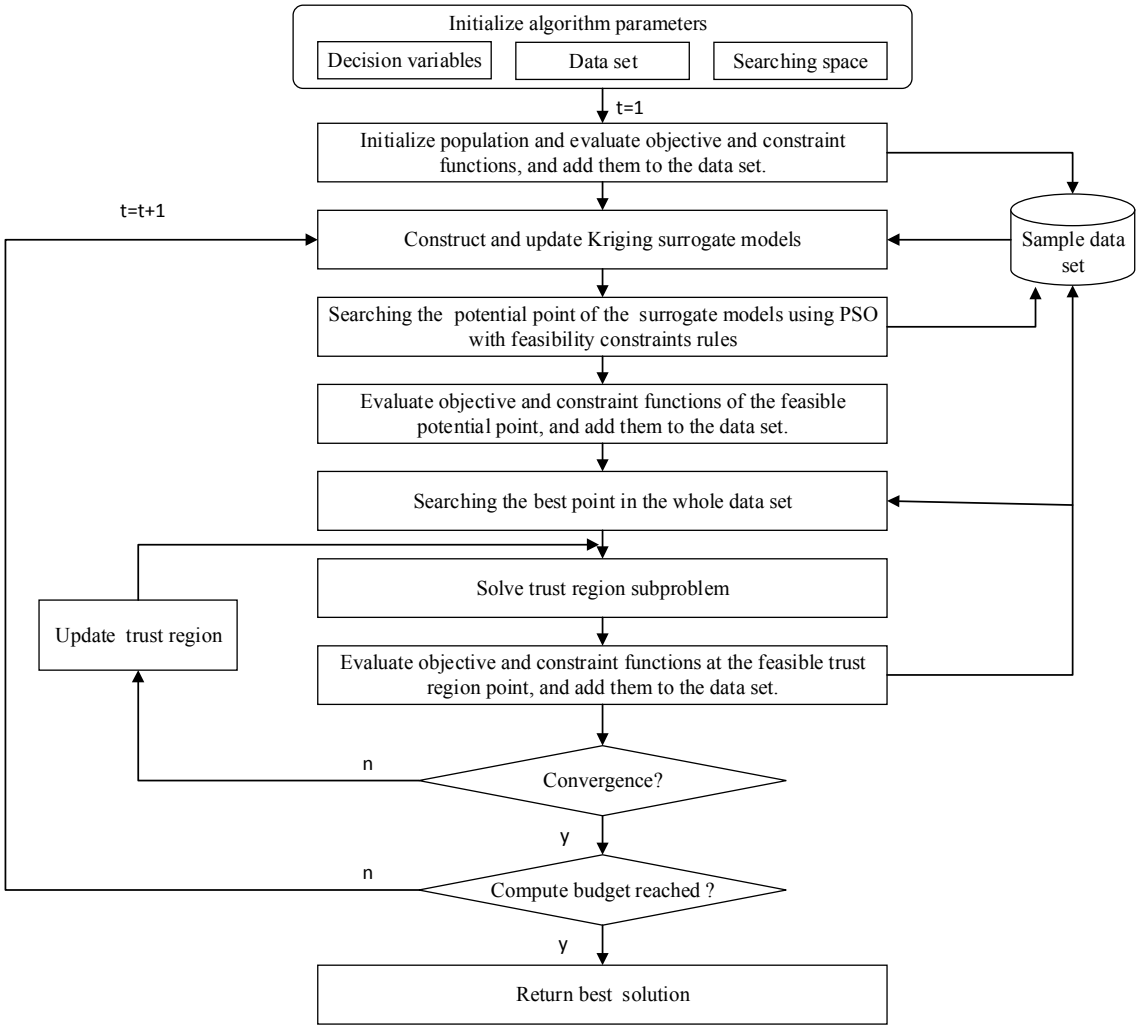

Fig. 1 Flowchart of main steps of TRSALS algorithm

The RBF-based trust-region (RBF-TR) search algorithm proceeds as follows:

Procedure *RBF-TR Algorithm*

Input: $D_t = \{x_{i,t}, f_{i,t}, g_{i,t}, i = 1,2,\cdots N\}$, initial searching space (with radius R), design parameters λ, feasible space A
Output: the best solution
1: **Begin**
2: Randomly select a point X_{t-1} in the searching space Ψ, and let $t = 1$
3: while *RBF-TR is* not convergenced
4: $\Delta f \leftarrow f(x_{t-1}) - f(x_t)$
5: if $\Delta f > 0$,then
6: $x_c \leftarrow x_t$
7: else
8: $x_c \leftarrow x_{t-1}$
9: end
10: $r \leftarrow GetTRFactor(f(x_{t-1}), f(x_t), \tilde{f}(x_t))$
11: $\delta_t \leftarrow \max\{Update(r, x_t, x_{t-1}), \lambda R\} \cap A$
12: $\psi_t \leftarrow [x_c - \delta_t, x_c + \delta_t]$
13: $S_k \leftarrow Latin(x_c, \psi_t)$
14: $\tilde{x}_t \leftarrow PSO: RBF(S_t)$ with feasibility constraint rules
15: end while
16: return $\tilde{x}_t$
17: end
18: End Procedure

Unlike a traditional trust-region algorithm, the RBF-TR algorithm utilizes the decreasing information of the objective function to scale the sampling space, so that the searching population can quickly converge to the global point. Regarding the RBF-based trust-region search, one should first determine the center point x_c in the sampling space. If the value of the original objective function decreases, that is, $\Delta y > 0$, then the current optimal solution x_t is taken as x_c; otherwise, the last optimal solution x_{t-1} is taken. Second, according to the search results, one can easily obtain the trust factor r as shown in Eq. (7), and then the trust-region radius is scaled following Eq. (8). Finally, boundary adjustment of the trust-region sampling space is conducted. The adjustment is conducive to improving the surrogate model accuracy in the trust region, avoiding falling into the local optimum, thus providing an effective search space:

$$r = \frac{f(x_{t-1}) - f(x_t)}{f(x_{t-1}) - \tilde{f}(x_t)} \tag{7}$$

where $f(x)$ is the objective function, $\tilde{f}(x)$ the trust-region approximate function, and t the generation counter:

$$\delta_t = \begin{cases} \max\{c1\|x_t - x_{t-1}\|, \lambda R\}, r < r1 \\ \max\{\min(c2\|x_t - x_{t-1}\|, \sigma), \lambda R\}, r > r2 \\ \max\{\|x_t - x_{t-1}\|, \lambda R\}, r1 \le r \le r2 \end{cases} \tag{8}$$

where $c1$ and $c2$ are parameters in the searching process, R is the initial search space, λ a minimum boundary control parameter, σ the upper bound of the trust-region radius, and $r1$ and $r2$ are the respective lower and upper bounds of the trust factors.

IV. Case Study

Two thousand groups of typical industrial steady-state operating data in the actual production process were collected as sample data to calibrate a xylene distillation unit with 68 layers of trays. According to the temperature distribution of the column, the column is divided into two sections. In the first section (from the 1st to the 32nd stage), namely, the 1st, 5th, 8th,10th, 15th, 18th, 26th, and 30th, the range of the efficiency is set as [0.80, 0.95], and is obtained by a simulation testing model under the typical operating conditions. In the other section, the range is [0.25, 0.45], and four key measuring points of the tray are selected, namely, the 35th, 40th, 60th, and 64th stages. The Murphree efficiency of the tray of the fractionation unit is determined by the TRSALS algorithm according to the objective and constraint functions as shown in Eq. (2). To verify the performance of the proposed algorithm, two evolutionary metrics are defined, that is, phenotypical diversity (*PDM*) and genotypical diversity (*GDM*), to evaluate the convergence metrics in the search process. *PDM* and *GDM* are defined as follows:

$$PDM = aff_{\min} / aff_{avg} \tag{9}$$

$$GDM = (\overline{E} - E_{\min})/(E_{\max} - E_{\min}) \tag{10}$$

where aff_{avg} and $aff_{\min}$ are the average and minimum fitness values of the population in the current generation, respectively; $\overline{E}$ is the average Euclidean distance between all individuals in the current generation; and $E_{\max}$ and $E_{\min}$ denote the maximum and minimum Euclidean distances of the population, respectively. *PDM* and *GDM* both belong to the interval [0,1], and the following three conclusions are those of the convergence of the algorithm in the evolutionary process:
If $0 < PDM \le 0.9$ and $GDM \ge 0.1$, the algorithm is in the searching state.
If $PDM \ge 0.9$ and $GDM < 0.1$, the algorithm tends to converge.
If $PDM \cong 1$ and $GDM = 0$, the algorithm is in the convergence state.

To verify the convergence performance of the TRSALS algorithm, it is compared with a Kriging surrogate-only algorithm. The parameter settings of the proposed algorithms are the following. The population size N is set to 100, $c1 = 0.80$, $c2 = 1.15$, $r1$=0.25, $r2$=0.85, $\lambda = 0.1$, and $R = 0.8$. The Kriging and RBF surrogate models used in this work are implemented using the SURROGATES toolbox [19]. The termination criteria set in this work is the maximum generation set to 500. Figures 2 and 3 show the *PDM* and *GDM* curves for two algorithms iterated for 500 generations. As shown in Fig. 2, compared with the Kriging surrogate-only algorithm, the *PDM* value of TRSALS is small in the early stage, and increases near to "1" in the late stage of the searching period. This indicates that TRSALS can better keep gene segments in the searching process and converge to the optimal point in the limited time. Note further that the *GDM* value of TRSALS is within the range [0.3,0.6] in the searching stage, while decreasing quickly in the late convergent stage. This means that TRSALS can well balance the convergence and diversity of the population during the run.

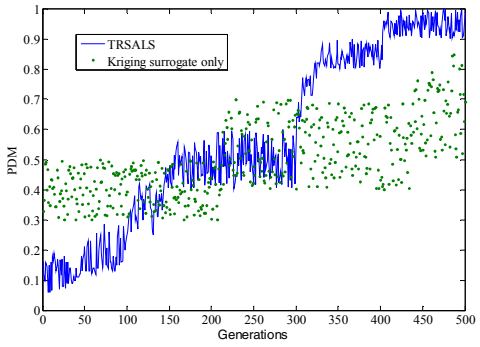

Fig. 2 *PDM* curve of the algorithms during the run

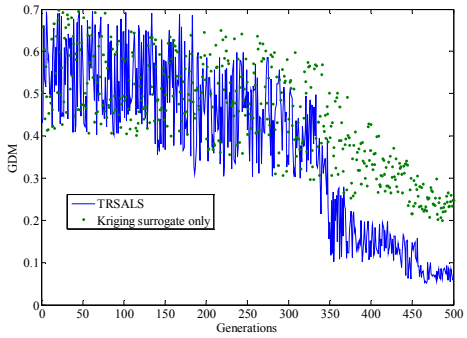

Fig.3 *GDM* curves of the algorithms during the run

To evaluate the prediction performance of the proposed algorithm, fitting experiments were performed and the mean-square error (MSE) and mean average percentage error (MAPE) performance metrics for prediction accuracy evaluation were defined, which are defined as follows:

$$MSE = \frac{1}{n}\sum_{i=1}^{n}\left|T_i - \hat{T}_i\right| \tag{11}$$

$$MAPE = \frac{1}{n}\sum_{i=1}^{n}\left|(T_i - \hat{T}_i)/T_i\right| \times 100\% \tag{12}$$

where T_i and $\hat{T}_i$ are the actual and predicted values of the output and n the number of tray test points; n = 12 was chosen in this study. The MSE and MAPE values of the TRSALS Kriging surrogate-only, and original distillation-only -based algorithms for 20 trials were calculated, and the statistical results are shown in Tables I and II. Figure 4 shows the fitting results of these two algorithms for the tray temperature distribution. From Tables I and II and Figure 4, it can be seen that the calculated tray temperatures of TRSALS are more consistent with the measured temperatures.

After estimating the tray Murphree efficiencies, the distillation model was then established and used to predict the tower top and bottom production. Table III displays the calculated and measured values of the main products under the steady-state operation. It can be seen from Table III that the output production of TRSALS is more consistent with the distillation measured one. This indicates that TRSALS exhibits higher accuracy than Kriging surrogate-only algorithms.

Table I. MSE for each method performing 20 trials for testing temperature points

MSE	***Kriging surrogate only***	***TRSALS***
Mean	2.825	1.15
Max	3.638	2.37
Min	1.342	0.87

Table II. MAPE for each method performing 20 trials for testing temperature points

MAPE	***Kriging surrogate only***	***TRSALS***
Mean	1.35%	0.56%
Max	1.94%	0.88%
Min	0.96%	0.31%

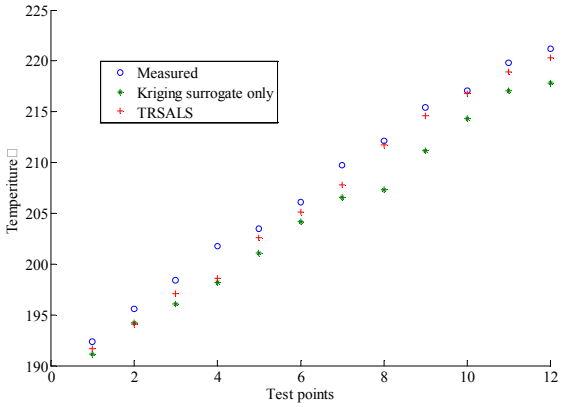

Fig. 4 Comparison of calculated tray temperatures and measured values

Table III. Comparison of calculated and measured values for products

Distillation unit		***Measured value***	***Kriging surrogate only***	***TRSALS***
		kmol/h	***kmol/h***	***kmol/h***
Tower top products	TOL	28.2	24.1	26.9
	PX	721.3	703.6	715.4
	MX	2192.5	2096.1	2167.2
	OX	613.1	601.2	609.4
	EB	251.2	241.2	245.9
	NA	153.2	148.5	150.2
Tower bottom products	PMET	61.6	59.2	60.3
	1,2,4-BZ	41.3	40.2	42.3
	1,3,5-BZ	32.2	33.9	32.7
	OET	18.1	22.2	19.4
	C9A	6.2	8.2	6.0

V. CONCLUSIONS

In the current study, a TRSALS method was proposed to estimate the tray efficiencies of industrial distillation columns on the basis of operating data. The Murphree efficiencies were determined by solving a constraint optimization problem. A Kriging surrogate combined with a trust-region local search approach was introduced to solve this problem, and its performance was outstanding compared with that of Kriging surrogate-only algorithm.

ACKNOWLEDGMENT

This work is supported in part by the Natural Science Foundation of China (61773225, 61803214).

REFERENCES

[1] R. Taylor, R. Krishna, Multi-component Mass Transfer, John Wiley Inc., New York, 1993.

[2] E.E. Ludwig, Applied Process Design for Chemical and Petrochemical Plants, Gulf, Texas, 1997.

[3] Mittal V., Zhang J. , Yang X., Xu Q. E3 Analysis for Crude and Vacuum Distillation System.Chemical Engineering & Technology, 2011, 34 (11):1854-1863.

[4] Mark L., Michael N. RTO: An overview and assessment of current practice. Journal of Process Control. 2011, 21(6): 874-884.

[5] Lluvia M. Ochoa E. and Megan J. Optimization of Heat-Integrated Crude Oil Distillation Systems. Part I: The Distillation Model. Industrial & Engineering Chemistry Research. 2015, 54: 4988-5000.

[6] Ye Z., QIAN Z., Luo N. Atmospheric tower energy optimization based on EGO. Journal of Chemical Industry and Engineering(China), 2014, 65(12):4929-4934.

[7] American Institute of Chemical Engineers. Bubble Tray Design Manual; AIChE: New York, 1958.

[8] American Institute of Chemical Engineers Research Committee. Tray Efficiencies in Distillation Columns, AIChE: New York, 1958.

[9] Chan, H.; Fair, J. R. Prediction of point efficiencies on sieve trays. 1. Binary systems. Ind. Eng. Chem. Process Des. Dev. 1984, 23 (4): 814-824.

[10] Prado, M.; Fair, J. R. Fundamental model for the prediction of sieve tray efficiency. Ind. Eng. Chem. Res. 1990, 29 (6):1031-1046.

[11] Garcia, J. A.; Fair, J. R. A fundamental model for the prediction of distillation sieve tray efficiency. 1. Database development. Ind. Eng. Chem. Res. 2000, 39 (6):1809-1820.

[12] Garcia, J. A.; Fair, J. R. A fundamental model for the prediction of distillation aieve tray wfficiency. 2. Model development and validation. Ind. Eng. Chem. Res. 2000, 39 (6):1818-1832.

[13] Domingues, T. L.; Secchi, A. R.; Mendes, T. F. Overall efficiency evaluation of commercial distillation columns with valve and dualflow trays. AIChE J. 2010, 56 (9): 2323-2336.

[14] O'Connell, H. E. Plate efficiency of fractionating columns and absorbers. Trans. Am. Inst. Chem. Eng. 1946, 42:741-756.

[15] Olivier, E.; Eldridge, R. B. Prediction of the trayed distillation column mass-transfer performance by neural networks. Ind. Eng. Chem. Res. 2002, 41 (14): 3436-3445.

[16] Luo, Na, Qian, Feng, Ye, Zhen-Cheng. Estimation of Mass-Transfer Efficiency for Industrial Distillation Columns, Industrial & Engineering Chemistry Research, 2012.

[17] Shi X.H. , Qian F. A Multi-agent Artificial Immune Network Algorithm for Estimation Tray Efficiencies of Distillation Unit. Chinese Journal of Chemical Engineering. 2012, 20(6): 1148-1153.

[18] Shi xuhua, Qianfeng. Multi-Agent Immune Network Algorithm Based Murphree Efficiency Determination for the Distillation Column. Journal of Bionic Engineering, 2011.8(2): 181-190.

[19] F. Viana and T. Goel, Surrogates toolbox user's guide, http://fchegury.googlepages. com, Tech. Rep., 2010.